Journal of Computational and Applied Mathematics 343 (2018) 12–25

Contents lists available at ScienceDirect

Journal of Computational and Applied Mathematics

journal homepage: www.elsevier.com/locate/cam

Parameter determination for Tikhonov regularization problems in general form☆

Y. Park [a], L. Reichel [b], G. Rodriguez [c,*], X. Yu [d]

[a] Department of Mathematical Science, Kent State University, Kent, OH 44240, USA
[b] Department of Mathematical Sciences, Kent State University, Kent, OH 44242, USA
[c] Dipartimento di Matematica e Informatica, Università di Cagliari, viale Merello 92, 09123 Cagliari, Italy
[d] Department of Mathematical Sciences, Kent State University, North Canton, OH 44720, USA

ARTICLE INFO

Article history:
Received 10 August 2017
Received in revised form 30 January 2018

MSC:
65F10
65F22
65R30

Keywords:
Ill-posed problem
Tikhonov regularization
TGSVD
Noise level estimation
Heuristic parameter choice rule

ABSTRACT

Tikhonov regularization is one of the most popular methods for computing an approximate solution of linear discrete ill-posed problems with error-contaminated data. A regularization parameter $\lambda > 0$ balances the influence of a fidelity term, which measures how well the data are approximated, and of a regularization term, which dampens the propagation of the data error into the computed approximate solution. The value of the regularization parameter is important for the quality of the computed solution: a too large value of $\lambda > 0$ gives an over-smoothed solution that lacks details that the desired solution may have, while a too small value yields a computed solution that is unnecessarily, and possibly severely, contaminated by propagated error. When a fairly accurate estimate of the norm of the error in the data is known, a suitable value of λ often can be determined with the aid of the discrepancy principle. This paper is concerned with the situation when the discrepancy principle cannot be applied. It then can be quite difficult to determine a suitable value of λ. We consider the situation when the Tikhonov regularization problem is in general form, i.e., when the regularization term is determined by a regularization matrix different from the identity, and describe an extension of the COSE method for determining the regularization parameter λ in this situation. This method has previously been discussed for Tikhonov regularization in standard form, i.e., for the situation when the regularization matrix is the identity. It is well known that Tikhonov regularization in general form, with a suitably chosen regularization matrix, can give a computed solution of higher quality than Tikhonov regularization in standard form.

1. Introduction

We are concerned with the solution of minimization problems of the form

$$\min_{\mathbf{x}\in\mathbb{R}^n} \|A\mathbf{x} - \mathbf{b}\|, \tag{1.1}$$

where $\|\cdot\|$ denotes the Euclidean norm, $A \in \mathbb{R}^{m\times n}$ is an ill-conditioned matrix whose singular values "cluster" at the origin, and the data vector $\mathbf{b} \in \mathbb{R}^m$ is contaminated by an unknown error $\mathbf{e} \in \mathbb{R}^m$ that may stem from measurement inaccuracies

☆ Version January 30, 2018.

* Corresponding author.
E-mail addresses: ypark7@kent.edu (Y. Park), reichel@math.kent.edu (L. Reichel), rodriguez@unica.it (G. Rodriguez), xyu3@kent.edu (X. Yu).

https://doi.org/10.1016/j.cam.2018.04.049
0377-0427/

and discretization error. Thus, $\mathbf{b} = \mathbf{b}_{\text{exact}} + \mathbf{e}$. We are interested in computing the solution $\mathbf{x}_{\text{exact}}$ of minimal Euclidean norm of the least-squares problem with error-free data vector,

$$\min_{\mathbf{x}\in\mathbb{R}^n} \|A\mathbf{x} - \mathbf{b}_{\text{exact}}\|,$$

associated with (1.1). The desired solution $\mathbf{x}_{\text{exact}}$ will be referred to as the *exact solution*. Since $\mathbf{b}_{\text{exact}}$ is not known, we seek to determine an approximation of $\mathbf{x}_{\text{exact}}$ by computing a suitable approximate solution of (1.1).

Least-squares problems of the form (1.1) arise in many areas of science and engineering. They are commonly referred to as discrete ill-posed problems, because they usually stem from the discretization of a linear ill-posed problem, such as a Fredholm integral equation of the first kind; see, e.g., [1].

Due to the ill-conditioning of the matrix A and the error $\mathbf{e}$ in the data vector $\mathbf{b}$, straightforward solution of the least-squares problem (1.1) generally does not give a meaningful approximation of $\mathbf{x}_{\text{exact}}$. Therefore, the minimization problem (1.1) is commonly replaced by a penalized least-squares problem of the form

$$\min_{\mathbf{x}\in\mathbb{R}^n}\{\|A\mathbf{x} - \mathbf{b}\|^2 + \lambda^2\|L\mathbf{x}\|^2\}. \tag{1.2}$$

This replacement is known as Tikhonov regularization. The parameter $\lambda > 0$ is the regularization parameter that balances the influence of the first term (the fidelity term) and the second term (the regularization term), which is determined by the regularization matrix $L \in \mathbb{R}^{p\times n}$. Here p is an arbitrary positive integer.

The purpose of the regularization term is to damp undesired components of the minimal-norm least-squares solution of (1.1). The minimization problem (1.2) is said to be in *standard form* when L is the identity matrix I, otherwise the minimization problem is said to be in *general form*. We are interested in Tikhonov regularization in general form, because for a suitable choice of regularization matrix $L \neq I$ the solution of (1.2) can be a much better approximation of $\mathbf{x}_{\text{exact}}$ than the solution of (1.2) with $L = I$; see, e.g., [2,3] for computed examples.

Common choices of the matrix L, when A stems from a uniform discretization of a Fredholm integral equation defined on an interval, are the bidiagonal rectangular matrix

$$L' = \frac{1}{2}\begin{bmatrix} 1 & -1 & & & 0 \\ & 1 & -1 & & \\ & & \ddots & \ddots & \\ 0 & & & 1 & -1 \end{bmatrix} \in \mathbb{R}^{(n-1)\times n} \tag{1.3}$$

and the tridiagonal rectangular matrix

$$L'' = \frac{1}{4}\begin{bmatrix} -1 & 2 & -1 & & & 0 \\ & -1 & 2 & -1 & & \\ & & \ddots & \ddots & \ddots & \\ 0 & & & -1 & 2 & -1 \end{bmatrix} \in \mathbb{R}^{(n-2)\times n}. \tag{1.4}$$

When, instead, A is obtained by discretizing a Fredholm integral equation in a uniform manner on a square, such as in image restoration, the regularization matrix

$$L = \begin{bmatrix} I_n \otimes L' \\ L' \otimes I_n \end{bmatrix}, \tag{1.5}$$

is commonly used; see, e.g., [4,5]. Here I_n denotes the identity matrix of order n and $\otimes$ stands for the Kronecker product. Many other regularization matrices have been proposed in the literature; see, e.g., [6–10].

The parameter determination approach of this paper can be applied to any regularization matrix $L \in \mathbb{R}^{p\times n}$ that satisfies

$$\mathcal{N}(A) \cap \mathcal{N}(L) = \{\mathbf{0}\}, \tag{1.6}$$

where $\mathcal{N}(M)$ denotes the null space of the matrix M. When (1.6) holds, the Tikhonov minimization problem (1.2) has the unique solution

$$\mathbf{x}_\lambda = (A^TA + \lambda^2 L^TL)^{-1}A^T\mathbf{b} \tag{1.7}$$

for any $\lambda > 0$, where the superscript ^{T} denotes transposition.

The value of the regularization parameter λ determines how well the solution $\mathbf{x}_\lambda$ of (1.2) approximates $\mathbf{x}_{\text{exact}}$ and how sensitive $\mathbf{x}_\lambda$ is to the error $\mathbf{e}$ in the available data vector $\mathbf{b}$. Assume for the moment that the norm $\|\mathbf{e}\| > 0$ is known and that the (unavailable) linear system of equations

$$A\mathbf{x} = \mathbf{b}_{\text{exact}} \tag{1.8}$$

is consistent. Then the discrepancy principle prescribes that the regularization parameter $\lambda > 0$ be chosen so that

$$\|A\mathbf{x}_\lambda - \mathbf{b}\| = \tau\|\mathbf{e}\|, \tag{1.9}$$

where $\tau > 1$ is a user-specified constant independent of $\|\mathbf{e}\|$; see [1,11] for discussions on this parameter choice method. It easily can be shown that there is a unique positive value of λ such that the solution (1.7) of (1.2) satisfies (1.9) for reasonable values of $\|\mathbf{e}\|$; see below.

We are interested in the common situation when no estimate of $\|\mathbf{e}\|$ is available. Parameter choice methods for this situation are commonly referred to as "heuristic", because they may fail in certain situations; see [1]. A large number of heuristic parameter choice methods have been proposed in the literature due to the importance of being able to determine a suitable value of the regularization parameter when the discrepancy principle cannot be used; see, e.g., [12–23]. These methods include the L-curve criterion, generalized cross validation, and the quasi-optimality principle.

Most heuristics parameter choice methods have been developed for the situation when the regularization matrix L in (1.2) is the identity matrix. We are concerned with the situation when $L \in \mathbb{R}^{p\times n}$ is a fairly general matrix such that (1.6) holds. It is the purpose of this paper to extend the Comparison of Solutions Estimator (COSE) method for determining a suitable value for the regularization parameter for Tikhonov regularization problems in standard form described in [19] to Tikhonov regularization problems in general form (1.2).

Section 2 describes the COSE method for Tikhonov minimization problems (1.2) that are small enough to allow the computation of the Generalized Singular Value Decomposition (GSVD) of the matrix pair (A, L). The availability of this decomposition makes it easy to solve the Tikhonov minimization problem (1.2) and determine a value of the regularization parameter $\lambda > 0$ such that the norm of the residual error $\|A\mathbf{x}_\lambda - \mathbf{b}\|$ achieves a prescribed value. Moreover, knowledge of the GSVD allows the inexpensive computation of a regularized approximate solution of (1.1) with the aid of the Truncated Generalized Singular Value Decomposition (TGSVD); see, e.g., [11,24]. Let $k \geq 1$ be the truncation index of the TGSVD method and denote the associated approximate solution of (1.1) by $\mathbf{x}_k$; see Section 2 for details on the definition of $\mathbf{x}_k$. Define the associated residual vector

$$\mathbf{r}_k = \mathbf{b} - A\mathbf{x}_k.$$

We consider $\mathbf{r}_k$ an error-vector and determine the value of the regularization parameter $\lambda = \lambda_k$ in (1.2) so that the associated Tikhonov solution $\mathbf{x}_{\lambda_k}$ of (1.7) satisfies (1.9) with $\tau\|\mathbf{e}\|$ replaced by $\|\mathbf{r}_k\|$. We then compute the smallest k-value, denoted by $k_{\min}$, that minimizes $k \to \|\mathbf{x}_k - \mathbf{x}_{\lambda_k}\|$ and use $\mathbf{x}_{k_{\min}}$ or $\mathbf{x}_{\lambda_{k_{\min}}}$ as approximations of $\mathbf{x}_{\text{exact}}$. Computed examples reported in [19] show this approach to compute an approximation of $\mathbf{x}_{\text{exact}}$ to be competitive with other available methods when $L = I$.

Section 3 is concerned with Tikhonov minimization problems (1.2) with matrices A and L that are too large to make the computation of the GSVD of the matrix pair (A, L) attractive or feasible. The matrices A and L are then first reduced to small or medium size, before the GSVD of the reduced matrices is computed. Several reduction methods are available in the literature; see, e.g., [3,5,25–27]. We discuss two methods for reducing Tikhonov regularization problems (1.2) with large matrices A and L to a Tikhonov regularization problem with small matrices. The methods differ in their handling of $\mathcal{N}(L)$. Section 4 describes a few computed examples and Section 5 contains concluding remarks.

2. A GSVD-based COSE method

Assume that the matrices $A \in \mathbb{R}^{m\times n}$ and $L \in \mathbb{R}^{p\times n}$ in (1.2) satisfy (1.6) and $m \geq n \geq p$, with m small enough to make the evaluation of the GSVD of the matrix pair (A, L) feasible. Then the GSVD furnishes decompositions of the form

$$A = U\begin{bmatrix}\Sigma & 0\\ 0 & I_{n-p}\end{bmatrix}Z^{-1}, \qquad L = V\begin{bmatrix}M & 0\end{bmatrix}Z^{-1}, \tag{2.1}$$

where the matrices $U \in \mathbb{R}^{m\times n}$ and $V \in \mathbb{R}^{p\times p}$ have orthonormal columns, $Z \in \mathbb{R}^{n\times n}$ is nonsingular, and the diagonal matrices

$$\Sigma = \operatorname{diag}[\sigma_1, \sigma_2, \ldots, \sigma_p] \in \mathbb{R}^{p\times p}, \qquad M = \operatorname{diag}[\mu_1, \mu_2, \ldots, \mu_p] \in \mathbb{R}^{p\times p}$$

have nonnegative diagonal entries ordered according to

$$0 = \sigma_1 = \cdots = \sigma_{p-\ell} < \sigma_{p-\ell+1} \leq \cdots \leq \sigma_p \leq 1, \qquad 1 \geq \mu_1 \geq \cdots \geq \mu_p \geq 0.$$

They are normalized so that $\sigma_i^2 + \mu_i^2 = 1$ for $i = 1, 2, \ldots, p$. The requirement (1.6) secures the existence of the nonsingular matrix Z. We may assume that the regularization matrix $L \in \mathbb{R}^{p\times n}$ in (1.2) satisfies $n \geq p$, because otherwise we compute its QR factorization $L = QR$, where $Q \in \mathbb{R}^{p\times n}$ has orthonormal columns and $R \in \mathbb{R}^{n\times n}$ is upper triangular, and replace L by R in (1.2).

A discussion on the computation of the GSVD is provided by Bai [28]; see also [29]. Here the inequality $m \geq n$ is not imposed. We required this inequality above for ease of exposition. The computation of the GSVD of a pair of matrices of moderate size is quite expensive. A simplification of the computations that reduces the count of arithmetic floating point operations is described in [2]. Recently, a modification of the decomposition (2.1) aimed to make an analogue of the matrix Z better conditioned has been discussed in [30].

Truncated GSVD (TGSVD) is a popular regularization method for the solution of discrete ill-posed problems (1.1) when a regularization matrix $L \neq I$ is used; see, e.g., [11,24]. Let $U = [\mathbf{u}_1, \ldots, \mathbf{u}_n]$ and $Z = [\mathbf{z}_1, \ldots, \mathbf{z}_n]$ be the matrices in (2.1). Substituting the decomposition (2.1) of A into (1.1) yields the simple minimization problem

$$\min_{\mathbf{y}\in\mathbb{R}^n}\left\|\begin{bmatrix}\Sigma & 0\\ 0 & I_{n-p}\end{bmatrix}\mathbf{y} - U^T\mathbf{b}\right\|, \tag{2.2}$$

where $\mathbf{y} = [y_1, y_2, \ldots, y_n]^T = Z^{-1}\mathbf{x}$. We remark that the regularization matrix L affects both the diagonal entries of Σ and the matrix U.

The TGSVD method restricts the solution of the minimization problem (2.2) to vectors $\mathbf{y}$ whose $p-k$ first entries, $y_1, y_2, \ldots, y_{p-k}$, vanish. These components are associated with the $p-k$ smallest diagonal elements of Σ. The parameter k is a discrete regularization parameter.

We obtain the solution of the so restricted minimization problem

$$\mathbf{y}_k = \left[0, \ldots, 0, \frac{\mathbf{u}_{p-k+1}^T\mathbf{b}}{\sigma_{p-k+1}}, \ldots, \frac{\mathbf{u}_p^T\mathbf{b}}{\sigma_p}, \mathbf{u}_{p+1}^T\mathbf{b}, \ldots, \mathbf{u}_n^T\mathbf{b}\right]^T,$$

which defines the approximate solution

$$\mathbf{x}_k = Z\mathbf{y}_k = \sum_{i=p-k+1}^{p} \frac{\mathbf{u}_i^T\mathbf{b}}{\sigma_i}\,\mathbf{z}_i + \sum_{i=p+1}^{n} (\mathbf{u}_i^T\mathbf{b})\,\mathbf{z}_i \tag{2.3}$$

of the least-squares problem (1.1), where $1 \le k \le \ell$. The approximate solution $\mathbf{x}_k$ only depends on the k largest diagonal entries of Σ. The last sum in the right-hand side represents the solution component in $\mathcal{N}(L)$.

The GSVD (2.1) allows us to express the Tikhonov solution (1.7) in the form

$$\mathbf{x}_\lambda = \sum_{i=1}^{p} \frac{\sigma_i\,\mathbf{u}_i^T\mathbf{b}}{\sigma_i^2 + \lambda^2\mu_i^2}\,\mathbf{z}_i + \sum_{i=p+1}^{n} (\mathbf{u}_i^T\mathbf{b})\,\mathbf{z}_i. \tag{2.4}$$

When the GSVD (2.1) of the matrix pair (A, L) is available, the TGSVD and Tikhonov solutions (2.3) and (2.4), respectively, are inexpensive to evaluate for different values of the regularization parameters k and λ. This is the basis of the COSE method. Introduce the residual norms associated with the TGSVD solutions $\mathbf{x}_k$,

$$\rho_k = \|A\mathbf{x}_k - UU^T\mathbf{b}\|, \qquad k = 1, 2, \ldots, \ell. \tag{2.5}$$

For each $k = 1, 2, \ldots, \ell$, we determine a Tikhonov solution (2.4) that corresponds to the residual error norm ρ_k. We use the orthogonal projector UU^T in (2.5) to achieve better performance for inconsistent problems (1.1) and problems with $m \gg n$. It follows from (2.1) that the range of A is a subset of the range of U. Therefore,

$$\|A\mathbf{x}_k - \mathbf{b}\|^2 = \|A\mathbf{x}_k - UU^T\mathbf{b}\|^2 + \|(I - UU^T)\mathbf{b}\|^2,$$

and no choice of the regularization parameter k can reduce the last term in the right-hand side.

Using the GSVD (2.1) and letting $\tau = 1/\lambda^2$, we can express the equation

$$\|A\mathbf{x}_\lambda - UU^T\mathbf{b}\|^2 = \rho_k^2$$

as a zero-finding problem for the function

$$f(\tau) = \sum_{j=1}^{p} \frac{\mu_j^4(\mathbf{u}_j^T\mathbf{b})^2}{(\sigma_j^2\tau + \mu_j^2)^2} - \rho_k^2. \tag{2.6}$$

It can easily be shown that this function has a unique zero. Newton's method applied to determine this zero can be expressed as

$$\tau_{q+1} = \tau_q + \frac{1}{2}\left[\sum_{j=1}^{p} \frac{\mu_j^4(\mathbf{u}_j^T\mathbf{b})^2}{(\sigma_j^2\tau_q + \mu_j^2)^2} - \rho_k^2\right] \cdot \left[\sum_{j=1}^{p} \frac{\sigma_j^2\mu_j^4(\mathbf{u}_j^T\mathbf{b})^2}{(\sigma_j^2\tau_q + \mu_j^2)^3}\right]^{-1}.$$

We remark that when $L = I$ and $\mu_j = 1$ for all j, and the σ_j are the singular values of A, the above iterations simplify to those used in [19]. Let $\tau_* > 0$ denote the computed zero of (2.6). Then $\lambda_k = \tau_*^{-1/2}$ gives the value of the regularization parameter for the Tikhonov solution (2.4).

Evaluate for $k = 1, 2, \ldots, \ell$ the quantities

$$\delta_k = \|\mathbf{x}_{\lambda_k} - \mathbf{x}_k\|, \tag{2.7}$$

and let $k_{\min}$ denote the index of the minimizer of the sequence $\delta_1, \delta_2, \ldots, \delta_\ell$. In case the minimizer is not unique, we let $k_{\min}$ be the smallest minimizer. When $k_{\min} = 1, 2$, we also consider the smallest minimizer of the sequence $\delta_3, \delta_4, \ldots, \delta_\ell$. If the latter has index $k > 3$, then we set $k_{\min} = k$. Our reason for doing this is that the sequence of the δ_k may exhibit a false local minimum at the very beginning, due to the fact that, e.g., the underregularized vectors $\mathbf{x}_{\lambda_1}$ and $\mathbf{x}_1$ may be close to each other, without λ_1 being a suitable choice of the regularization parameter λ.

We may use either the TGSVD solution $\mathbf{x}_{k_{\min}}$ or the Tikhonov solution $\mathbf{x}_{\lambda_{k_{\min}}}$ as approximations of the desired solution $\mathbf{x}_{\text{exact}}$ of (1.1). When the system (1.8) is consistent and $m = n$ in (2.1), the quantity

$$\rho_{k_{\min}} = \|A\mathbf{x}_{\lambda_{k_{\min}}} - UU^T\mathbf{b}\| \tag{2.8}$$

typically furnishes a quite accurate estimate of the norm of the error $\mathbf{e}$ in the data vector $\mathbf{b}$. The regularization parameters $k_{\min}$ and $\lambda_{k_{\min}}$ determined by the following algorithm typically are appropriate also for inconsistent problems (1.1).

Algorithm 1 Comparison of solution estimator for $L \neq I$.

Input: Matrices $A \in \mathbb{R}^{m\times n}$, $L \in \mathbb{R}^{p\times n}$, data vector $\mathbf{b} \in \mathbb{R}^m$
Output: Tikhonov regularization parameter, TGSVD truncation index

1: Compute the GSVD (2.1) of the matrix pair (A, L)
2: Compute the TGSVD solutions (2.3) $\mathbf{x}_k$, $k = 1, \ldots, \ell$
3: **for** $k = 1, \ldots, \ell$ **do**
4: Compute residual norm $\rho_k = \|A\mathbf{x}_k - UU^T\mathbf{b}\|$
5: Compute Tikhonov regularization parameter λ_k by determining the zero of the function (2.6)
6: Compute the Tikhonov solution (2.4)

$$\mathbf{x}_{\lambda_k} = \sum_{j=1}^{p} \frac{\sigma_j}{\sigma_j^2 + \lambda_k^2\mu_j^2}(\mathbf{u}_j^T\mathbf{b})\mathbf{x}_j + \sum_{j=p+1}^{n} (\mathbf{u}_j^T\mathbf{b})\mathbf{x}_j$$

7: Compute $\delta_k = \|\mathbf{x}_{\lambda_k} - \mathbf{x}_k\|$
8: **end for**
9: $k_{\min} = \arg\min_{k=1,\ldots,\ell} \delta_k$
10: **if** $k_{\min} \leq 2$ **then**
11: $k_2 = \arg\min_{k=k_{\min}+1,\ldots,k_{\max}} \delta_k$
12: **if** $k_2 > k_{\min} + 1$ **then**
13: $k_{\min} = k_2$
14: **end if**
15: **end if**
16: The TGSVD truncation index is $k_{\min}$, the Tikhonov regularization parameter is $\lambda_{k_{\min}}$.

Algorithm 1 computes the value $k_{\min}$ of the truncation index for the TGSVD method as well as the corresponding value $\lambda_{k_{\min}}$ of the regularization parameter for Tikhonov regularization. In the numerical experiments, we display these parameters as well as the estimate (2.8) of the norm of the error in the data vector $\mathbf{b}$ furnished by the computed Tikhonov solution. Computed examples presented in Section 4 show this estimate to be quite accurate for many computed examples when the system (1.8) is consistent.

3. Large-scale problems

It is prohibitively expensive to compute the GSVD of a pair of large matrices. Tikhonov regularization problems (1.2) with large matrices A and L have to be reduced to problems of small size before the COSE method of Section 2 can be applied. Many reduction methods have been described in the literature; see, e.g., [3,25]. We will show examples with a method described in [26], that first reduces A by applying $r \ll \min\{m, n\}$ steps of Golub–Kahan bidiagonalization with initial vector $\mathbf{b}$. Generically, this yields the decompositions

$$AW_r = \widetilde{W}_{r+1}B_{r+1,r}, \qquad A^T\widetilde{W}_r = W_rB_{r,r}^T, \tag{3.1}$$

where the matrices $W_r = [\mathbf{w}_1, \mathbf{w}_2, \ldots, \mathbf{w}_r] \in \mathbb{R}^{n\times r}$ and $\widetilde{W}_{r+1} = [\widetilde{\mathbf{w}}_1, \widetilde{\mathbf{w}}_2, \ldots, \widetilde{\mathbf{w}}_{r+1}] \in \mathbb{R}^{m\times(r+1)}$ have orthonormal columns with $\widetilde{\mathbf{w}}_1 = \mathbf{b}/\|\mathbf{b}\|$. The matrix $\widetilde{W}_r$ is made up of the first r columns of $\widetilde{W}_{r+1}$, and $B_{r+1,r}$ is lower bidiagonal with positive diagonal and subdiagonal entries,

$$B_{r+1,r} := \begin{bmatrix} \rho_1 & & & & 0 \\ \sigma_2 & \rho_2 & & & \\ & \ddots & \ddots & & \\ & & \sigma_{r-1} & \rho_{r-1} & \\ & & & \sigma_r & \rho_r \\ 0 & & & & \sigma_{r+1} \end{bmatrix} \in \mathbb{R}^{(r+1)\times r}.$$

It has the leading principal submatrix $B_{r,r} \in \mathbb{R}^{r\times r}$; see, e.g., [29] for details. We assume that r is chosen small enough so that the decompositions (3.1) with the stated properties exist. The value of r used in computations, generally, is not large; in particular, $r \ll n$.

We seek a solution of (1.2) in the subspace range(W_r). Thus, we solve the Tikhonov minimization problem

$$\min_{\mathbf{y}\in\mathbb{R}^r}\{\|AW_r\mathbf{y} - \mathbf{b}\|^2 + \lambda^2\|LW_r\mathbf{y}\|^2\}. \tag{3.2}$$

It follows from (1.6) that this problem has a unique solution for any $\lambda > 0$.

Introduce the QR factorization

$$LW_r = Q_r R_r, \tag{3.3}$$

i.e., the matrix $Q_r \in \mathbb{R}^{p\times r}$ has orthonormal columns and $R_r \in \mathbb{R}^{r\times r}$ is upper triangular, or upper trapezoidal in case $\operatorname{rank}(LW_r) < r$. Here we assume that $r \leq p$. Using the factorization (3.3) and the decompositions (3.1), we can express (3.2) as

$$\min_{\mathbf{y}\in\mathbb{R}^r}\{\|B_{r+1,r}\mathbf{y} - \|\mathbf{b}\|\mathbf{e}_1\|^2 + \lambda^2\|R_r\mathbf{y}\|^2\}, \tag{3.4}$$

where $\mathbf{e}_1 = [1, 0, \ldots, 0]^T$ denotes the first axis vector. The matrices in (3.4) are small and the COSE method of Section 2 can be applied to this reduced Tikhonov minimization problem. The overall procedure is described in Algorithm 2.

We remark that when an initial number of bidiagonalization steps r is chosen, and subsequently is increased to be able to compute a more accurate approximation of the desired solution $\mathbf{x}_{\text{exact}}$, the QR factorization (3.3) has to be updated. Daniel et al. [31] describe efficient formulas for this purpose.

Algorithm 2 COSE for $L \neq I$ for large-scale problems based on partial Golub–Kahan bidiagonalization.

Input: Matrices $A \in \mathbb{R}^{m\times n}$, $L \in \mathbb{R}^{p\times n}$, data vector $\mathbf{b} \in \mathbb{R}^m$, number of steps r_{steps}, max number of steps $N_{\max}$
Output: GK/TGSVD and Tikhonov parameters $r_{\min}$, $\lambda_{r_{\min}}$, and corresponding regularized solutions $\mathbf{x}_{r_{\min}}$, $\mathbf{x}_{\lambda_{r_{\min}}}$

$\widetilde{\mathbf{w}}_1 = \mathbf{b}/\|\mathbf{b}\|$
$r = 0$
repeat
  $r = r + r_{\text{steps}}$
  Perform r_{steps} steps of Golub–Kahan (GK) bidiagonalization, obtaining matrices $\widetilde{W}_{r+1}$, W_r, and $B_{r+1,r}$
  Compute the compact QR factorization of LW_r
  $\widetilde{\mathbf{b}} = \|\mathbf{b}\|\mathbf{e}_1 \in \mathbb{R}^{r+1}$
  Apply Algorithm 1 to the projected least squares problem $\min \|B_{r+1,r}\mathbf{y} - \widetilde{\mathbf{b}}\|$ with regularization matrix R, obtaining the truncation index $r_{\min}$, the Tikhonov parameter $\lambda_{r_{\min}}$, and the regularized solutions $\mathbf{y}_{r_{\min}}$, $\mathbf{y}_{\lambda_{r_{\min}}}$
until $(r_{\min} < 0.75 \cdot r)$ **or** $(r > N_{\max})$ **or** (GK stops for breakdown)
The TGSVD truncation index is $r_{\min}$, the Tikhonov parameter is $\lambda_{r_{\min}}$
$\mathbf{x}_{r_{\min}} = W_r\mathbf{y}_{r_{\min}}$, $\mathbf{x}_{\lambda_{r_{\min}}} = W_r\mathbf{y}_{\lambda_{r_{\min}}}$

The solution method described above does not consider $\mathcal{N}(L)$ in the choice of solution subspace. The following, alternate, approach explicitly determines a solution component in $\mathcal{N}(L)$. This component is not damped by L. The approach is applicable when $\mathcal{N}(L)$ is known and has fairly small dimension, and guarantees that certain solution features represented by $\mathcal{N}(L)$ are not damped. It has previously been applied in several direct and iterative solution methods [26,32,33]. Let the orthonormal columns of the matrix $\breve{W}_s \in \mathbb{R}^{n\times s}$ span $\mathcal{N}(L)$ and introduce the QR factorization,

$$A\breve{W}_s = \breve{Q}_s\breve{R}_s,$$

where $\breve{Q}_s \in \mathbb{R}^{n\times s}$ has orthonormal columns and $\breve{R}_s \in \mathbb{R}^{s\times s}$ is upper triangular. Due to (1.6), the matrix $\breve{R}_s$ is nonsingular. Introduce the orthogonal projectors

$$P_{\breve{W}_s} = \breve{W}_s\breve{W}_s^T, \qquad P_{\breve{W}_s}^{\perp} = I - \breve{W}_s\breve{W}_s^T, \qquad P_{\breve{Q}_s} = \breve{Q}_s\breve{Q}_s^T, \qquad P_{\breve{Q}_s}^{\perp} = I - \breve{Q}_s\breve{Q}_s^T.$$

Then, using that $I = P_{\breve{W}_s} + P_{\breve{W}_s}^{\perp}$ and $P_{\breve{Q}_s}^{\perp}AP_{\breve{W}_s} = 0$, we obtain

$$\begin{aligned}\|A\mathbf{x} - \mathbf{b}\|^2 &= \|P_{\breve{Q}_s}A\mathbf{x} - P_{\breve{Q}_s}\mathbf{b}\|^2 + \|P_{\breve{Q}_s}^{\perp}A\mathbf{x} - P_{\breve{Q}_s}^{\perp}\mathbf{b}\|^2\\ &= \|P_{\breve{Q}_s}AP_{\breve{W}_s}\mathbf{x} - (P_{\breve{Q}_s}\mathbf{b} - P_{\breve{Q}_s}AP_{\breve{W}_s}^{\perp}\mathbf{x})\|^2 + \|P_{\breve{Q}_s}^{\perp}AP_{\breve{W}_s}^{\perp}\mathbf{x} - P_{\breve{Q}_s}^{\perp}\mathbf{b}\|^2.\end{aligned}$$

Substitution into (1.2) gives

$$\min_{\mathbf{x}\in\mathbb{R}^n}\{\|P_{\breve{Q}_s}AP_{\breve{W}_s}\mathbf{x} - (P_{\breve{Q}_s}\mathbf{b} - P_{\breve{Q}_s}AP_{\breve{W}_s}^{\perp}\mathbf{x})\|^2 + \|P_{\breve{Q}_s}^{\perp}AP_{\breve{W}_s}^{\perp}\mathbf{x} - P_{\breve{Q}_s}^{\perp}\mathbf{b}\|^2 + \lambda^2\|L\mathbf{x}\|^2\}.$$

Let $\mathbf{y} = \breve{W}_s^T\mathbf{x}$. Then

$$\|P_{\breve{Q}_s}AP_{\breve{W}_s}\mathbf{x} - (P_{\breve{Q}_s}\mathbf{b} - P_{\breve{Q}_s}AP_{\breve{W}_s}^{\perp}x)\| = \|\breve{R}_s\mathbf{y} - (\breve{Q}_s^T\mathbf{b} - \breve{Q}_s^TAP_{\breve{W}_s}^{\perp}\mathbf{x})\|. \tag{3.5}$$

Since $\breve{R}_s$ is nonsingular, we may for any $P_{\breve{W}_s}^{\perp}\mathbf{x}$ determine $\mathbf{y} \in \mathbb{R}^s$ so that the expression in the right-hand side of (3.5) vanishes. This determines the component $\breve{W}_s\mathbf{y}$ in $\mathcal{N}(L)$ of the solution of (1.2). The solution component in $\mathcal{N}(L)^{\perp}$ is $P_{\breve{W}_s}^{\perp}\mathbf{x}$, where $\mathbf{x}$ solves

$$\min_{\mathbf{x}\in\mathbb{R}^n}\{\|P_{\breve{Q}_s}^{\perp}AP_{\breve{W}_s}^{\perp}\mathbf{x} - P_{\breve{Q}_s}^{\perp}\mathbf{b}\|^2 + \lambda^2\|LP_{\breve{W}_s}^{\perp}\mathbf{x}\|^2\}.$$

Table 4.1
Discretized ill-conditioned test problems used in the numerical experiments.

Baart	Deriv2(2)	Foxgood	Gravity	Heat(1)
Hilbert	Lotkin	Phillips	Prolate	Shaw

We solve this projected minimization problem as described above, i.e., we apply r steps of Golub–Kahan bidiagonalization to the matrix $P^{\perp}_{\breve{Q}_s} A P^{\perp}_{\breve{W}_s}$. This yields (an approximation of) the component in $\mathcal{N}(L)^{\perp}$ of the solution $\mathbf{x}$ of (1.2), which allows us to determine $\mathbf{y} \in \mathbb{R}^s$ such that (3.5) vanishes and gives the solution component in $\mathcal{N}(L)$. We remark that since $P^{\perp}_{\breve{Q}_s} A P^{\perp}_{\breve{W}_s} = P^{\perp}_{\breve{Q}_s} A$, we may omit the projector $P^{\perp}_{\breve{W}_s}$. The matrix $P^{\perp}_{\breve{Q}_s} A$, of course, does not have to be explicitly formed. This splitting of the solution of (1.2) into components in $\mathcal{N}(L)$ and $\mathcal{N}(L)^{\perp}$ is attractive when the dimension of $\mathcal{N}(L)$ is not large. See Algorithm 3 for a summary of the method.

Algorithm 3 COSE for $L \neq I$ for large-scale problems based on partial Golub–Kahan bidiagonalization and the availability of a basis for the null space of L.

Input: Matrices $A \in \mathbb{R}^{m\times n}$, $L \in \mathbb{R}^{p\times n}$, $\breve{U} \in \mathbb{R}^{n\times s}$ whose columns are a basis for $\mathcal{N}(L)$, data vector $\mathbf{b} \in \mathbb{R}^m$, number of steps r_{steps}

Output: GK/TGSVD and Tikhonov parameters $r_{\min}$, $\lambda_{r_{\min}}$, and corresponding regularized solutions $\mathbf{x}_{r_{\min}}$, $\mathbf{x}_{\lambda_{r_{\min}}}$

1: Orthonormalize the basis for $\mathcal{N}(L)$ by the QR factorization $\breve{W}M = \breve{U}$
2: Compute the QR factorization $\breve{Q}\breve{R} = A\breve{W}$
3: Compute the projection $\breve{A} = A - \breve{Q}(\breve{Q}^T A)$
4: Compute the projection $\breve{\mathbf{b}} = \mathbf{b} - \breve{Q}(\breve{Q}^T \mathbf{b})$
5: Apply Algorithm 2 with input $\breve{A}$, L, $\breve{\mathbf{b}}$, and number of steps r_{steps}, obtaining the truncation index $r_{\min}$, the Tikhonov parameter $\lambda_{r_{\min}}$, and the regularized solutions $\mathbf{z}_{r_{\min}}$, $\mathbf{z}_{\lambda_{r_{\min}}}$. The matrix $\breve{A}$, of course, is not explicitly formed.
6: Solve the triangular linear system $\breve{R}\mathbf{y} = \breve{Q}^T(b - A\mathbf{z}_{r_{\min}})$
7: $\mathbf{z} = \breve{W}\mathbf{y}$
8: The TGSVD truncation index is $r_{\min}$, the Tikhonov parameter is $\lambda_{r_{\min}}$
9: $\mathbf{x}_{r_{\min}} = \mathbf{z}_{r_{\min}} + \mathbf{z}$, $\mathbf{x}_{\lambda_{r_{\min}}} = \mathbf{z}_{\lambda_{r_{\min}}} + \mathbf{z}$

4. Numerical example

In this section we investigate the performance of the proposed methods by means of selected ill-conditioned test problems, listed in Table 4.1. Most of them are contained in Hansen's Regularization Tools [34], except for the matrices Hilbert, Lotkin, and Prolate, which are constructed with the `gallery` function of MATLAB. Each problem from [34] is associated to a model solution $\mathbf{x}_{\text{exact}}$; for the `gallery` examples, we use the solution of the problem Baart from [34]. MATLAB functions that implement the algorithms described in this paper, as well as algorithms from [19], are available at the authors' home pages; see, e.g., http://bugs.unica.it/~gppe/soft/.

For each test problem, we first determine the noise-free data vector as $\mathbf{b}_{\text{exact}} = A\mathbf{x}_{\text{exact}}$; then the associated perturbed data vector $\mathbf{b}$ is obtained by

$$\mathbf{b} = \mathbf{b}_{\text{exact}} + \frac{\nu}{\sqrt{n}} \|\mathbf{b}_{\text{exact}}\| \mathbf{w},$$

where $\mathbf{w}$ is a vector whose components are normally distributed with zero mean and unit variance, and ν is the *noise level*.

Fig. 4.1 illustrates the performance of Algorithm 1. We consider the test problem Gravity from [34] with $m = n = 40$. The regularization matrix is chosen to be the discrete approximation of the first derivative L', defined in (1.3), and the noise level is $\nu = 10^{-2}$. For each value of the TGSVD truncation parameter $k = 1, 3, \ldots, 11$, we plot the exact solution $\mathbf{x}_{\text{exact}}$, the TGSVD solution $\mathbf{x}_k$ (2.3) and the associated Tikhonov solution $\mathbf{x}_{\lambda_k}$ (2.4). The last vector is obtained by minimizing the function (2.6) by Newton's method.

In this numerical example, as it happens in the majority of cases, the vectors $\mathbf{x}_k$ and $\mathbf{x}_{\lambda_k}$ are closest to each other when they best approximate the solution $\mathbf{x}_{\text{exact}}$. The minimum of the quantities δ_k (2.7) is achieved for $k = 5$, which also produces the least Euclidean norm error. This is shown by Fig. 4.2, which displays the values of the error

$$\|\mathbf{x}_k - \mathbf{x}_{\text{exact}}\| \tag{4.1}$$

and δ_k as functions of k.

To compare Algorithm 1 to other well-known methods for the estimation of the truncation parameter in TGSVD, we replicate for the new algorithm Experiment 4.1 from [19]. For each test problem in Table 4.1, we construct two "square"

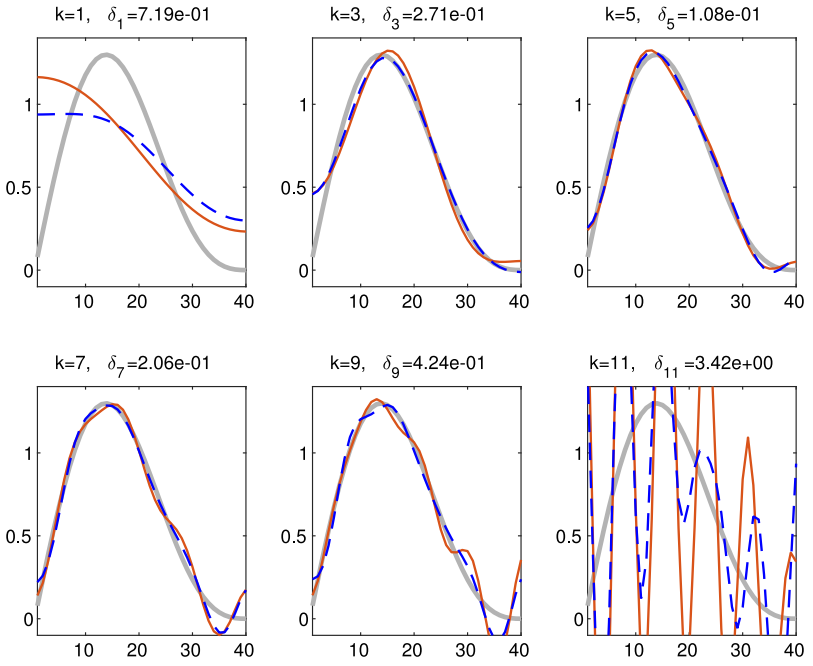

Fig. 4.1. Test problem GRAVITY, from [34], with $m = n = 40$, $L = L'$ given by (1.3), and $\nu = 10^{-2}$. The thick graphs represent the exact solution, the thin graphs show TGSVD solutions $\mathbf{x}_k$ for $k = 1, 3, \ldots, 11$, and the dashed graphs are the corresponding Tikhonov solutions $\mathbf{x}_{\lambda_k}$. Each plot reports the value of δ_k (2.7). The minimal δ_k, as well as the best approximation of $\mathbf{x}_{\text{exact}}$ in the Euclidean norm, are achieved for $k = 5$.

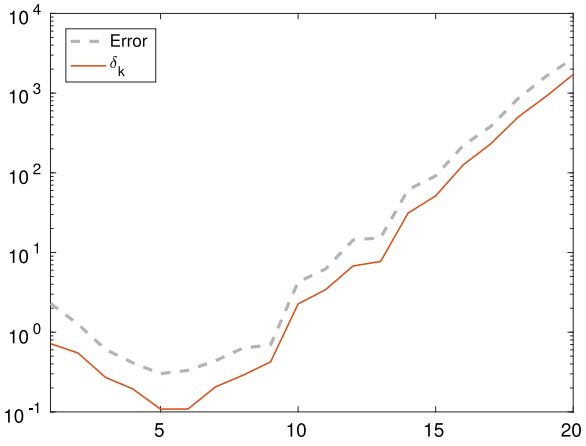

Fig. 4.2. The thick dashed graph represents the error (4.1) for the numerical experiment reported in Fig. 4.1, and the thin graph represents the values of δ_k (2.7), for $k = 1, 2, \ldots, 20$. The minima of both graphs are attained for $k = 5$.

discretizations, of size $n = 40$ and $n = 100$, respectively, and two "rectangular" ones, of size 80×40 and 200×100. The noise level is set to the values $\nu = 10^{-3}, 10^{-2}, 10^{-1}$, which are compatible with real-world applications, and each normally distributed noise vector $\mathbf{w}$ is generated 10 times. This procedure produces 600 square linear systems and 600 rectangular consistent systems.

To investigate the behavior of the methods also for inconsistent linear systems, we introduce a vector $\mathbf{q}$ that is orthogonal to the range of the over-determined matrix A. A multiple ϕ of $\mathbf{q}$ is then added to the right-hand side of the consistent system, to obtain

$$\mathbf{b}_{\text{exact}} = A\mathbf{x}_{\text{exact}} + \phi\,\mathbf{q}. \tag{4.2}$$

By repeating the above process with $\phi = 1$ and $\phi = 10$, we construct two sets of 600 rectangular inconsistent linear systems.

Table 4.2
Percentage of numerical experiments that lead to a regularized solution x_k such that (4.3) holds for $\rho = 2$ ($\rho = 5$), for TSVD with $L = L'$ given by (1.3) and different values of ϕ in (4.2).

Method	Square systems	Rectangular systems		
		$\phi = 0$	$\phi = 1$	$\phi = 10$
COSE	17%(2%)	19%(4%)	19%(4%)	22%(5%)
L-corner [18]	36%(18%)	39%(22%)	79%(59%)	84%(62%)
Res L-curve [35]	51%(30%)	63%(35%)	81%(64%)	83%(68%)
Regińska [36]	58%(30%)	32%(11%)	56%(36%)	46%(28%)
ResReg [22]	36%(4%)	27%(5%)	56%(36%)	46%(28%)
Quasiopt [34]	44%(22%)	34%(10%)	31%(10%)	27%(9%)
GCV [34]	49%(41%)	25%(13%)	43%(18%)	43%(21%)
Extrapolation [13]	61%(13%)	58%(19%)	56%(36%)	46%(28%)
Discrepancy [1]	23%(1%)	41%(3%)	69%(43%)	68%(49%)

Table 4.3
Percentage of numerical experiments that lead to a regularized solution x_k such that (4.3) holds for $\rho = 10$ ($\rho = 100$), for TSVD with $L = L'$ given by (1.3) and different values of ϕ in (4.2).

Method	Square systems	Rectangular systems		
		$\phi = 0$	$\phi = 1$	$\phi = 10$
COSE	1%(0%)	1%(0%)	2%(0%)	2%(0%)
L-corner [18]	16%(12%)	20%(15%)	45%(25%)	49%(35%)
Res L-curve [35]	23%(7%)	29%(17%)	53%(30%)	58%(39%)
Regińska [36]	20%(3%)	6%(0%)	24%(1%)	16%(0%)
ResReg [22]	0%(0%)	2%(0%)	24%(1%)	16%(0%)
Quasiopt [34]	16%(2%)	5%(0%)	5%(0%)	4%(0%)
GCV [34]	39%(35%)	12%(6%)	10%(1%)	12%(0%)
Extrapolation [13]	5%(1%)	4%(0%)	24%(1%)	16%(0%)
Discrepancy [1]	0%(0%)	1%(0%)	37%(36%)	47%(45%)

Let k_{best} be the truncation index that gives the least Euclidean error norm

$$E_{\text{best}} = \|\mathbf{x}_{k_{\text{best}}} - \mathbf{x}_{\text{exact}}\| = \min_k \|\mathbf{x}_k - \mathbf{x}_{\text{exact}}\|.$$

In Table 4.2 we record the percentage of numerical experiments that Algorithm 1, as well as a set of competing methods, produced an error larger than a certain multiple, $\rho > 1$, of the best error E_{best}. The methods considered besides COSE are well known; we give some references to the particular implementation we used: L-corner [18], Residual L-curve [35], Regińska criterion [36], Restricted Regińska criterion [22], Quasi-optimality [34], Generalized Cross Validation (GCV) [34], and Extrapolation [13]. The discrepancy principle selects the smallest index k such that

$$\|A\mathbf{x}_k - \mathbf{b}\|^2 \le (1.3\,\nu\,\|\mathbf{b}\|)^2 + \phi^2.$$

The first entry of columns 2 to 5 of Table 4.2 reports, for each method considered and with L defined by (1.3), the percentage of numerical experiments that lead to a regularized solution $\mathbf{x}_k$ such that

$$\|\mathbf{x}_k - \mathbf{x}_{\text{exact}}\| > \rho\, E_{\text{best}} \tag{4.3}$$

for $\rho = 2$, while the second entry (in parentheses) displays the same quantity in the case $\rho = 5$.

Table 4.3 reports the same results for the factors $\rho = 10$ and $\rho = 100$. Both tables show that the COSE approach is extremely effective in approximating the TGSVD regularization parameter. In particular, it is the only method, among the ones tested, to produce trustworthy estimates both for consistent and inconsistent problems. From this point of view, only the quasi-optimality criterion gives comparable results.

Similar remarks can be deduced from Tables 4.4 and 4.5, which reproduce analogous measurements of Tables 4.2 and 4.3 with the regularization matrix L'' (1.4). We conclude that the performance of the COSE method with $L \neq I$ is similar to that reported in [19] for Tikhonov regularization problems in standard form, that is, with $L = I$.

We turn to numerical experiments that illustrate the behavior of the COSE method when applied to large-scale problems, i.e., we discuss the performance of Algorithms 2 and 3. The first algorithm constructs a linear space of small dimension by the Golub–Kahan process, where the original problem is projected before applying Algorithm 1. No information about the null space of the regularization matrix L is required. Algorithm 3, on the other hand, requires a user to provide a basis of this null space. The availability of this basis makes it possible to decompose the given problem into a large-scale problem, whose solution is orthogonal to $\mathcal{N}(L)$ and which is solved by Algorithm 2, and a small problem which furnishes the component of the solution in the null space.

Fig. 4.3 is concerned with the solution of the test problem PHILLIPS from [34] of size 500×500, with noise level $\nu = 10^{-2}$ and $L = L''$. The plot on the left shows the Euclidean error norm produced by Algorithms 2 and 3 when k increases. The optimal values for the two methods are $k_2^{\text{opt}} = 7$ and $k_3^{\text{opt}} = 5$, respectively. The graphs on the right display the behavior of

Table 4.4
Percentage of numerical experiments that lead to a regularized solution x_k such that (4.3) holds for $\rho = 2$ ($\rho = 5$), for TSVD with $L = L''$ given by (1.4) and different values of ϕ in (4.2).

Method	Square systems	Rectangular systems		
		$\phi = 0$	$\phi = 1$	$\phi = 10$
COSE	21%(4%)	18%(5%)	18%(5%)	17%(5%)
L-corner [18]	63%(46%)	65%(51%)	78%(66%)	82%(70%)
Res L-curve [35]	60%(44%)	75%(57%)	83%(72%)	82%(69%)
Regińska [36]	31%(15%)	22%(8%)	32%(17%)	24%(11%)
ResReg [22]	23%(6%)	19%(1%)	32%(17%)	24%(11%)
Quasiopt [34]	34%(18%)	23%(9%)	21%(8%)	17%(6%)
GCV [34]	63%(59%)	22%(16%)	33%(18%)	24%(11%)
Extrapolation [13]	42%(19%)	33%(8%)	33%(17%)	24%(11%)
Discrepancy [1]	22%(3%)	24%(1%)	51%(39%)	55%(48%)

Table 4.5
Percentage of numerical experiments that lead to a regularized solution x_k such that (4.3) holds for $\rho = 10$ ($\rho = 100$), for TSVD with $L = L''$ given by (1.4) and different values of ϕ in (4.2).

Method	Square systems	Rectangular systems		
		$\phi = 0$	$\phi = 1$	$\phi = 10$
COSE	1%(0%)	3%(0%)	3%(0%)	3%(0%)
L-corner [18]	40%(32%)	48%(36%)	60%(42%)	61%(45%)
Res L-curve [35]	39%(23%)	52%(32%)	61%(39%)	59%(40%)
Regińska [36]	4%(0%)	4%(0%)	7%(0%)	0%(0%)
ResReg [22]	1%(0%)	0%(0%)	7%(0%)	0%(0%)
Quasiopt [34]	10%(0%)	4%(0%)	3%(0%)	0%(0%)
GCV [34]	57%(54%)	13%(5%)	8%(0%)	0%(0%)
Extrapolation [13]	5%(2%)	1%(0%)	7%(0%)	1%(0%)
Discrepancy [1]	0%(0%)	0%(0%)	38%(36%)	46%(45%)

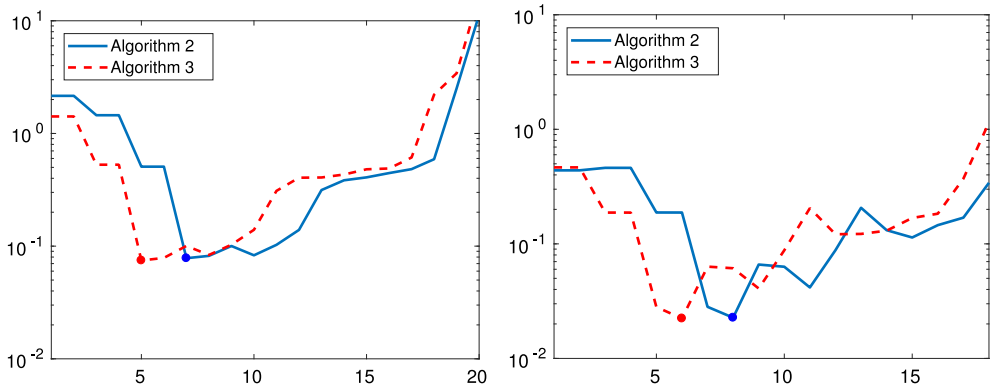

Fig. 4.3. Test problem PHILLIPS, from [34], with $m = n = 500$, $\nu = 10^{-2}$, $L = L''$, $k_2^{\text{opt}} = 7$, $k_3^{\text{opt}} = 5$, $k_2 = 8$, $k_3 = 6$. The errors (4.1) are plotted on the left and the δ_k on the right for $k = 1, 2, \ldots$.

the quantity δ_k (2.7), which is minimized by $k_2 = 8$ and $k_3 = 6$. The errors obtained with these parameter values are very close to the optimal error, and the approximate solutions determined by Algorithms 2 and 3 are close to the model solution, as the graphs on the left of Fig. 4.5 shows.

Fig. 4.4 illustrates a case when Algorithm 2 fails. The test problem is SHAW from [34]; the noise level and regularization matrix are the same as above. In this case, the trend of the δ_k is quite oscillatory and a false minimum at $k_2 = 4$ produces an over-regularized solution; see the graph on the right of Fig. 4.5. On the contrary, Algorithm 3 returns the optimal solution.

Algorithm 2 produces an incorrect solution also for the problem DERIV2 from [34]; see Fig. 4.6. Here, there is a different problem: the projected Krylov space does not contain a suitable approximation for the solution, as is testified by the slowly decaying error curve, whose minimum is well approximated by the algorithm. The resulting solution is under-regularized, as the left plot of Fig. 4.8 shows, while Algorithm 3 gives an accurate approximation.

In the above example the model solution is only approximately in $\mathcal{N}(L'')$. In Fig. 4.7 we analyze the case of a nontrivial solution which is exactly contained in the null space. We consider the model solution $\mathbf{x}_{\text{exact}}$ with components

$$x_i = \sin \frac{4\pi(i-1)}{n}, \qquad i = 1, \ldots, n,$$

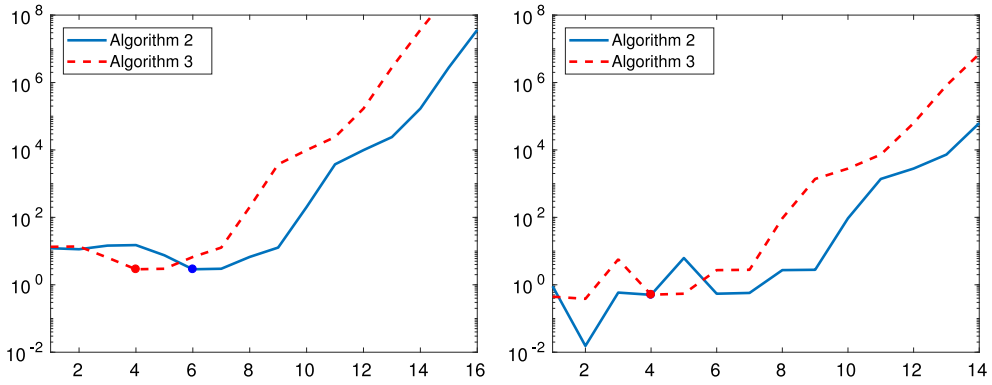

Fig. 4.4. Test problem Shaw from [34] with $m = n = 500$, $\nu = 10^{-2}$, $L = L''$, $k_2^{\text{opt}} = 6$, $k_3^{\text{opt}} = 4$, $k_2 = 4$, $k_3 = 4$. The errors (4.1) are displayed on the left and the δ_k on the right for $k = 1, 2, \ldots$.

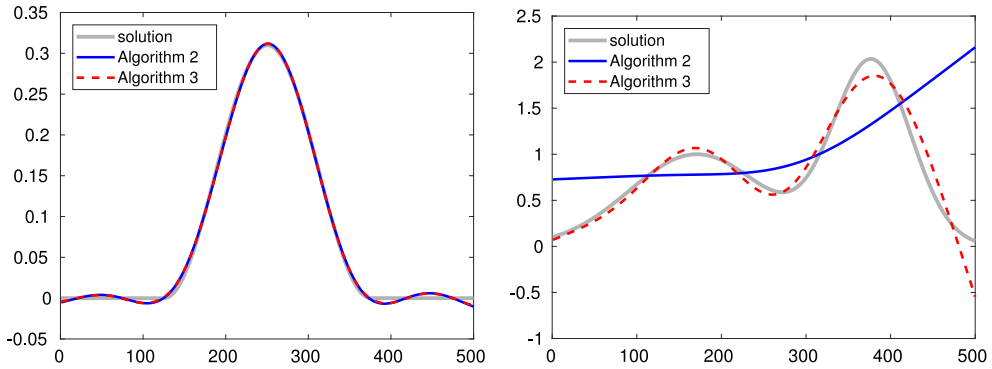

Fig. 4.5. Exact and computed approximate solutions for the numerical examples of Figs. 4.3 (left) and 4.4 (right).

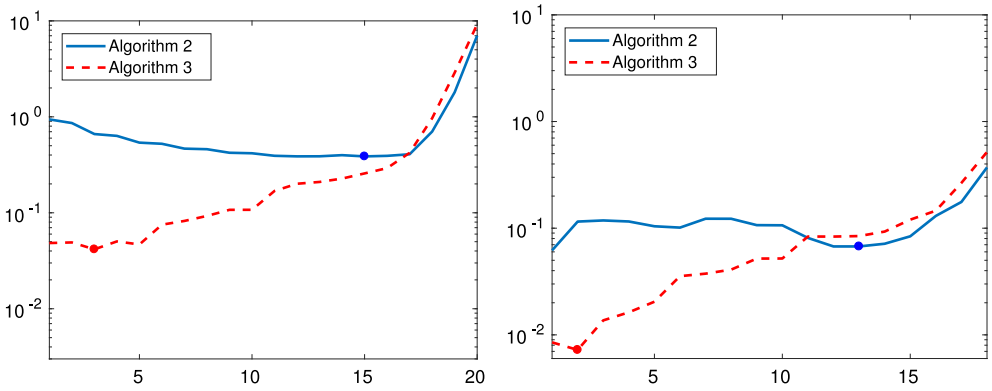

Fig. 4.6. Test problem Deriv2 from [34] with $m = n = 500$, $\nu = 10^{-2}$, $L = L''$, $k_2^{\text{opt}} = 15$, $k_3^{\text{opt}} = 3$, $k_2 = 13$, $k_3 = 2$. The errors (4.1) are shown on the left and the δ_k on the right for $k = 1, 2, \ldots$.

and choose $L = \frac{16\pi^2}{n^2} I + L''$. Both Algorithms 2 and 3 yield accurate approximations of $\mathbf{x}_{\text{exact}}$ for this problem, and the computed solutions are graphically indistinguishable from $\mathbf{x}_{\text{exact}}$, as the right plot in Fig. 4.8 shows.

To conclude, we consider the regularization matrix (1.5), and apply it to the solution of an image restoration problem, namely, the test problem Tomo from [34]. We fix the input parameter N to 32; this generates a linear system with $m = n = 1024$. The noise level is $\nu = 10^{-2}$.

The graphs for the errors and δ_k-values are shown in Fig. 4.9. Due to the very slow decay of the singular values of the coefficient matrix, we fixed the maximum number of iteration to 400. Both Algorithm 2 and Algorithm 3 are able to correctly

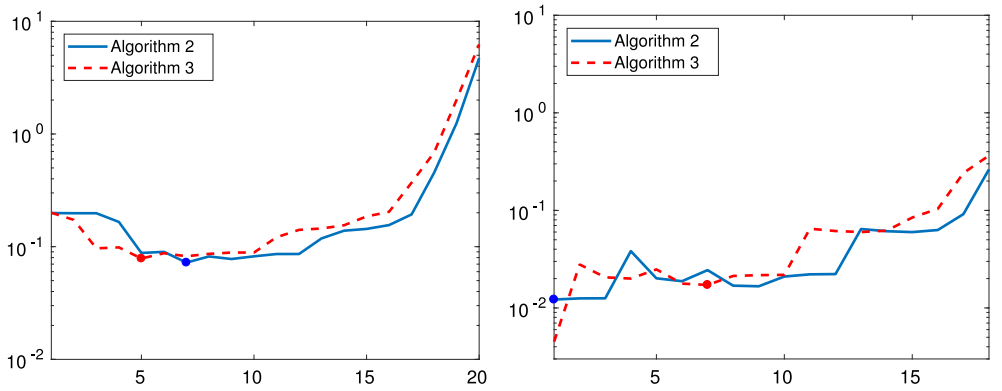

Fig. 4.7. Test problem Deriv2, from [34], with the "sin" solution, $m = n = 500$, $\nu = 10^{-2}$, $L = L''$, $k_2^{\text{opt}} = 7$, $k_3^{\text{opt}} = 5$, $k_2 = 1$, $k_3 = 7$. The errors (4.1) are depicted on the left and the δ_k on the right for $k = 1, 2, \ldots$.

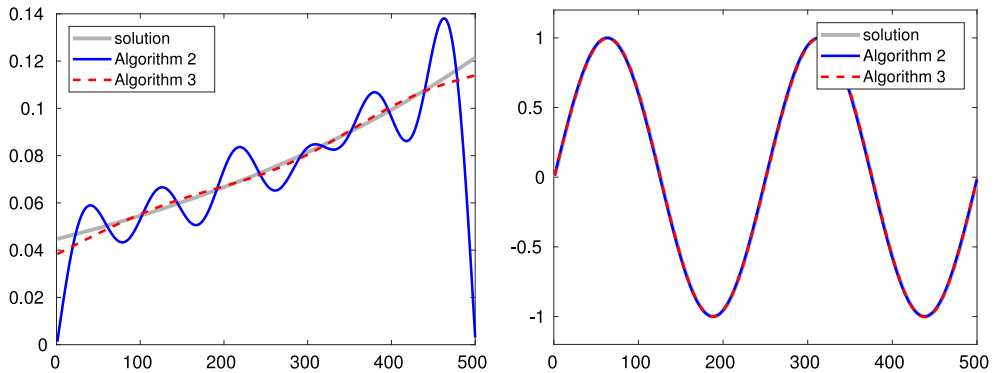

Fig. 4.8. Exact and computed approximate solutions for the numerical examples of Figs. 4.6 and 4.7.

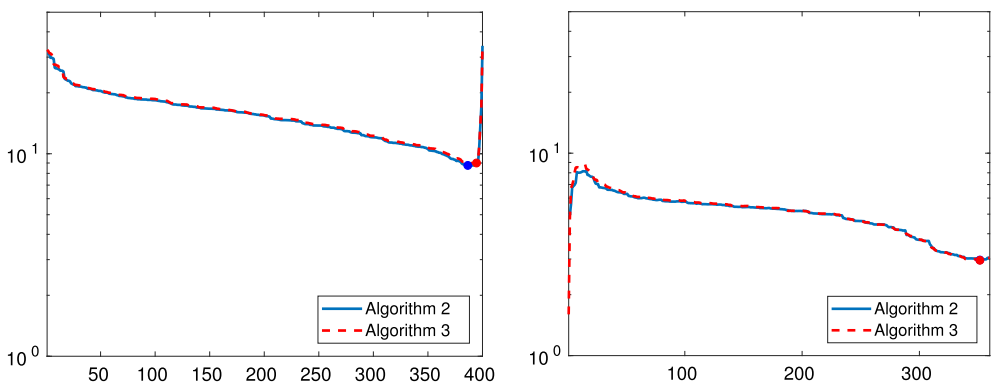

Fig. 4.9. Test problem Tomo, from [34], with $m = n = 1024$, $\nu = 10^{-2}$, L defined by (1.5), $k_2^{\text{opt}} = 386$, $k_3^{\text{opt}} = 386$, $k_2 = 360$, $k_3 = 360$. The errors (4.1) are shown on the left and the δ_k on the right for $k = 1, 2, \ldots$.

estimate the optimal regularization parameter within this range. This is confirmed by the plots of the solutions, reported in Fig. 4.10.

5. Conclusion

It is well known that the use of a regularization matrix $L \neq I$ in (1.2) can yield better approximations of the desired solution $\mathbf{x}_{\text{exact}}$ than $L = I$. However, while there are many heuristic techniques available for determining a suitable value of the regularization parameter when $L = I$, much less attention has been paid to the development of heuristic methods for

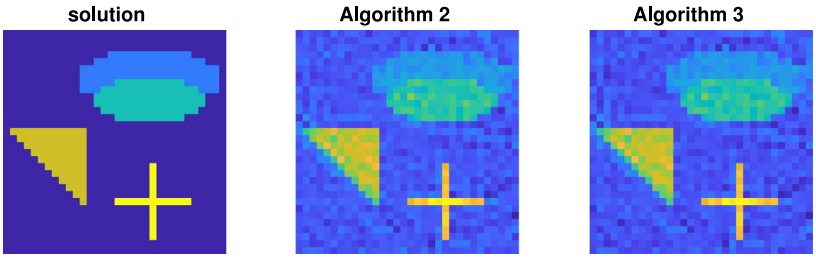

Fig. 4.10. Exact and computed approximate solutions for the numerical example of Fig. 4.9.

$L \neq I$. This paper describes three algorithms that can be applied for general matrices $L \in \mathbb{R}^{p\times n}$. One of these algorithms is well suited for problems of small to moderate size and two algorithms are suitable for use with large-scale problems. The latter algorithms differ in how the null space of L is handled; one of them requires the null space to be explicitly known. Computed examples illustrate the performance of the algorithms described and show them to be competitive.

Acknowledgments

The authors would like to thank a referee for comments that lead to clarifications of the presentation. Research of LR was supported in part by National Science Foundation (NSF) grants DMS-1729509 and DMS-1720259. Research of GR was partially supported by INdAM-GNCS. Part of this work was carried out during a visit to Cagliari by LR, supported by the Sardegna Ricerche Scientific School program.

References

[1] H.W. Engl, M. Hanke, A. Neubauer, Regularization of Inverse Problems, Kluwer, Dordrecht, 1996.
[2] L. Dykes, L. Reichel, Simplified GSVD computations for the solution of linear discrete ill-posed problems, J. Comput. Appl. Math. 255 (2013) 15–27.
[3] L. Reichel, X. Yu, Matrix decompositions for Tikhonov regularization, Electron. Trans. Numer. Anal. 43 (2015) 223–243.
[4] D. Calvetti, B. Lewis, L. Reichel, A hybrid GMRES and TV-norm based method for image restoration, in: F.T. Luk (Ed.), Advanced Signal Processing Algorithms, Architectures, and Implementations XII, in: Proceedings of the Society of Photo-Optical Instrumentation Engineers (SPIE), vol. 4791, The International Society for Optical Engineering, Bellingham, WA, 2002, pp. 192–200.
[5] M.E. Kilmer, P.C. Hansen, M.I. Español, A projection-based approach to general-form Tikhonov regularization, SIAM J. Sci. Comput. 29 (2007) 315–330.
[6] A. Bouhamidi, K. Jbilou, Sylvester Tikhonov-regularization methods in image restoration, J. Comput. Appl. Math. 206 (2007) 86–98.
[7] M. Donatelli, A. Neuman, L. Reichel, Square regularization matrices for large linear discrete ill-posed problems, Numer. Linear Algebra Appl. 19 (2012) 896–913.
[8] G. Huang, S. Noschese, L. Reichel, Regularization matrices determined by matrix nearness problems, Linear Algebra Appl. 502 (2016) 41–57.
[9] S. Noschese, L. Reichel, Inverse problems for regularization matrices, Numer. Algorithms 60 (2012) 531–544.
[10] L. Reichel, Q. Ye, Simple square smoothing regularization operators, Electron. Trans. Numer. Anal. 33 (2009) 63–83.
[11] P.C. Hansen, Rank-Deficient and Discrete Ill-Posed Problems, SIAM, Philadelphia, 1998.
[12] F. Bauer, M.A. Lukas, Comparing parameter choice methods for regularization of ill-posed problem, Math. Comput. Simulation 81 (2011) 1795–1841.
[13] C. Brezinski, G. Rodriguez, S. Seatzu, Error estimates for the regularization of least squares problems, Numer. Algorithms 51 (2009) 61–76.
[14] D. Calvetti, P.C. Hansen, L. Reichel, L-curve curvature bounds via Lanczos bidiagonalization, Electron. Trans. Numer. Anal. 14 (2002) 20–35.
[15] J.L. Castellanos, S. Gómez, V. Guerra, The triangle method for finding the corner of the L-curve, Appl. Numer. Math. 43 (2002) 359–373.
[16] C. Fenu, L. Reichel, G. Rodriguez, GCV for Tikhonov regularization via global Golub–Kahan decomposition, Numer. Linear Algebra Appl. 23 (2016) 467–484.
[17] C. Fenu, L. Reichel, G. Rodriguez, H. Sadok, GCV for Tikhonov regularization by partial SVD, BIT 57 (2017) 1019–1039.
[18] P.C. Hansen, T.K. Jensen, G. Rodriguez, An adaptive pruning algorithm for the discrete L-curve criterion, J. Comput. Appl. Math. 198 (2006) 483–492.
[19] M.E. Hochstenbach, L. Reichel, G. Rodriguez, Regularization parameter determination for discrete ill-posed problems, J. Comput. Appl. Math. 273 (2015) 132–149.
[20] S. Kindermann, Convergence analysis of minimization-based noise-level-free parameter choice rules for ill-posed problems, Electron. Trans. Numer. Anal. 38 (2011) 233–257.
[21] S. Kindermann, Discretization independent convergence rates for noise level-free parameter choice rules for the regularization of ill-conditioned problems, Electron. Trans. Numer. Anal. 40 (2013) 58–81.
[22] L. Reichel, G. Rodriguez, Old and new parameter choice rules for discrete ill-posed problems, Numer. Algorithms 63 (2013) 65–87.
[23] L. Reichel, G. Rodriguez, S. Seatzu, Error estimates for large-scale ill-posed problems, Numer. Algorithms 51 (2009) 341–361.
[24] P.C. Hansen, Regularization, GSVD and truncated GSVD, BIT 29 (1989) 491–504.
[25] S. Gazzola, P. Novati, M.R. Russo, On Krylov projection methods and Tikhonov regularization, Electron. Trans. Numer. Anal. 44 (2015) 83–123.
[26] M.E. Hochstenbach, L. Reichel, An iterative method for Tikhonov regularization with a general linear regularization operator, J. Integral Equations Appl. 22 (2010) 463–480.
[27] J. Lampe, L. Reichel, H. Voss, Large-scale Tikhonov regularization via reduction by orthogonal projection, Linear Algebra Appl. 436 (2012) 2845–2865.
[28] Z. Bai, The CSD, GSVD, their applications and computation, IMA preprint 958, Institute for Mathematics and its Applications, University of Minnesota, Minneapolis, MN, 1992.
[29] G.H. Golub, C.F. Van Loan, Matrix Computations, fourth ed., Johns Hopkins University Press, Baltimore, 2013.
[30] L. Dykes, S. Noschese, L. Reichel, Rescaling the GSVD with application to ill-posed problems, Numer. Algorithms 68 (2015) 531–545.
[31] J.W. Daniel, W.B. Gragg, L. Kaufman, G.W. Stewart, Reorthogonalization and stable algorithms for updating the Gram–Schmidt QR factorization, Math. Comp. 30 (1976) 772–795.

[32] J. Baglama, L. Reichel, Decomposition methods for large linear discrete ill-posed problems, J. Comput. Appl. Math. 198 (2007) 332–342.
[33] S. Morigi, L. Reichel, F. Sgallari, A truncated projected SVD method for linear discrete ill-posed problems, Numer. Algorithms 43 (2006) 197–213.
[34] P.C. Hansen, Regularization tools version 4.0 for MATLAB 7.3, Numer. Algorithms 46 (2007) 189–194.
[35] L. Reichel, H. Sadok, A new L-curve for ill-posed problems, J. Comput. Appl. Math. 219 (2008) 493–508.
[36] T. Regińska, A regularization parameter in discrete ill-posed problems, SIAM J. Sci. Comput. 17 (1996) 740–749.